QCD Phenomenology at High Energy

Bryan Webber

CERN & Univ. Cambridge

CERN Academic Training Lectures, October 2003

Lecture 2: e^+e^- & parton branching

- e^+e^- annihilation
  - Total cross section
  - Shape distributions
  - Jet fractions
- Parton branching
  - Kinematics
  - Splitting functions
  - Phase space
  - 4-jet angular distribution

e^+e^- annihilation cross section

- $e^+e^- \to \mu^+\mu^-$ is a fundamental electroweak processes. Same type of process, $e^+e^- \to q\bar{q}$, will produce hadrons. Cross sections are roughly proportional.

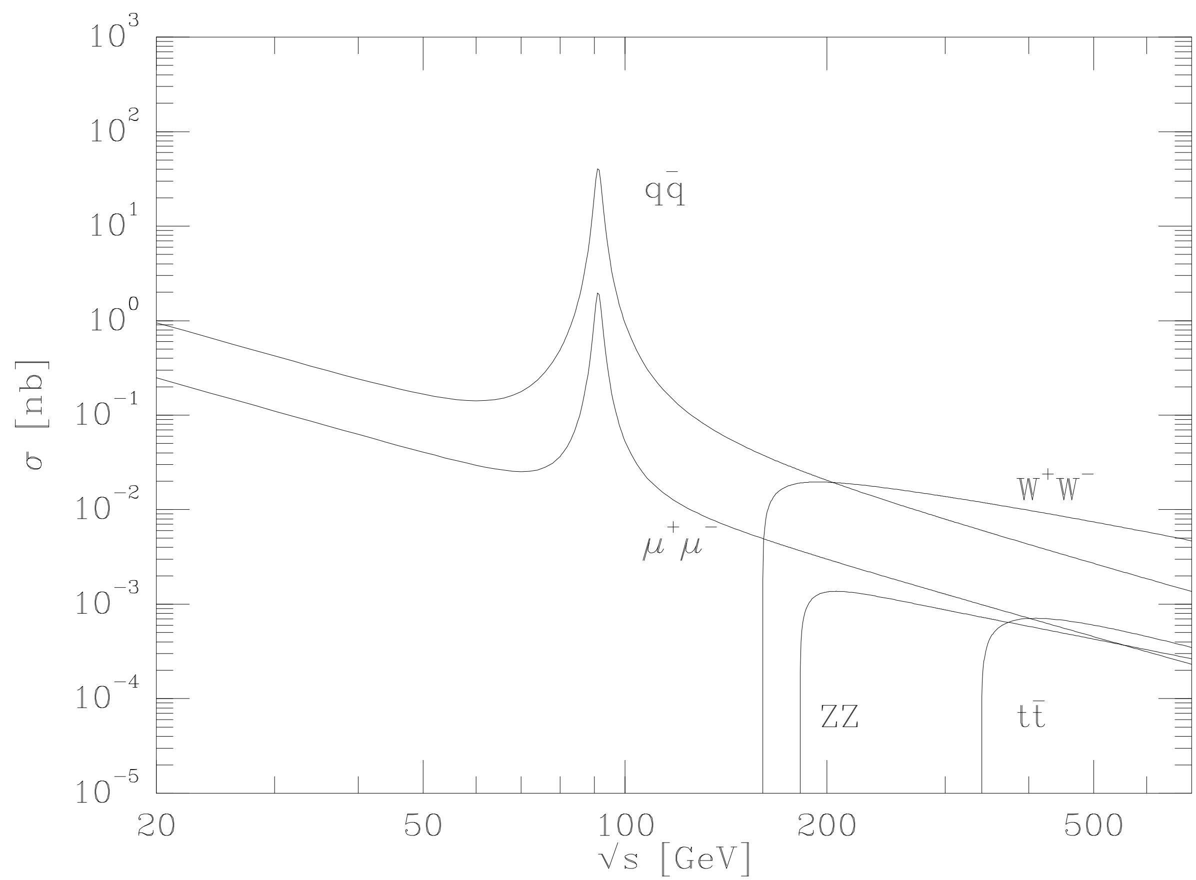

- Since formation of hadrons is non-perturbative, how can PT give hadronic cross section? This can be understood by visualizing event in space-time:
  - e^+ and e^- collide to form γ or Z^0 with virtual mass $Q = \sqrt{s}$. This fluctuates into $q\bar{q}$, $q\bar{q}g$,…, occupy space-time volume $\sim 1/Q$. At large Q, rate for this short-distance process given by PT.

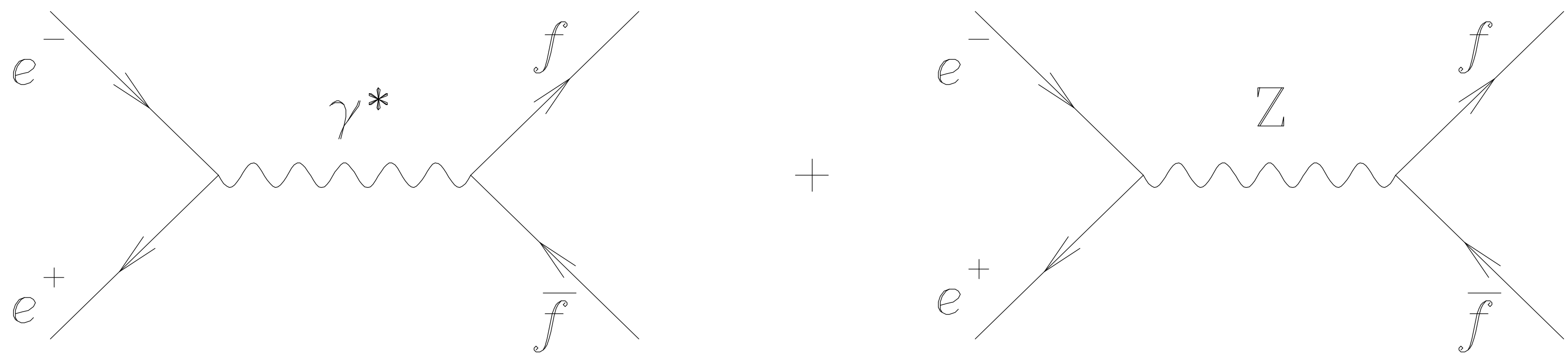

  - Subsequently, at much later time $\sim 1/\Lambda$, produced quarks and gluons form hadrons. This modifies outgoing state, but occurs too late to change original probability for event to happen.
- Well below Z^0, process $e^+e^- \to f\bar{f}$ is purely electromagnetic, with lowest-order (Born) cross section (neglecting quark masses)

$$\sigma_0 = \frac{4\pi\alpha^2}{3s} Q_f^2$$

Thus ($3 = N =$ number of possible $q\bar{q}$ colours)

$$R \equiv \frac{\sigma(e^+e^- \to \text{hadrons})}{\sigma(e^+e^- \to \mu^+\mu^-)} = \frac{\sum_q \sigma(e^+e^- \to q\bar{q})}{\sigma(e^+e^- \to \mu^+\mu^-)} = 3\sum_q Q_q^2 \,.$$

- On Z^0 pole, $\sqrt{s} = M_Z$, neglecting γ/Z interference

$$\sigma_0 = \frac{4\pi\alpha^2\kappa^2}{3\Gamma_Z^2}\,(a_e^2 + v_e^2)\,(a_f^2 + v_f^2)$$

where $\kappa = \sqrt{2}G_F M_Z^2/4\pi\alpha = 1/\sin^2(2\theta_W) \simeq 1.5$. Hence

$$R_Z = \frac{\Gamma(Z \to \text{hadrons})}{\Gamma(Z \to \mu^+\mu^-)} = \frac{\sum_q \Gamma(Z \to q\bar{q})}{\Gamma(Z \to \mu^+\mu^-)} = \frac{3\sum_q (a_q^2 + v_q^2)}{a_\mu^2 + v_\mu^2}$$

- Measured cross section is about 5% higher than σ_0, due to QCD corrections. For massless quarks, corrections to R and R_Z are equal. To $\mathcal{O}(\alpha_s)$ we have:

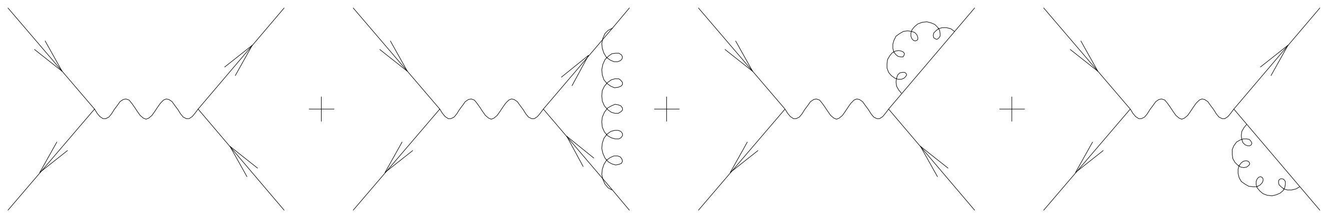

(a)

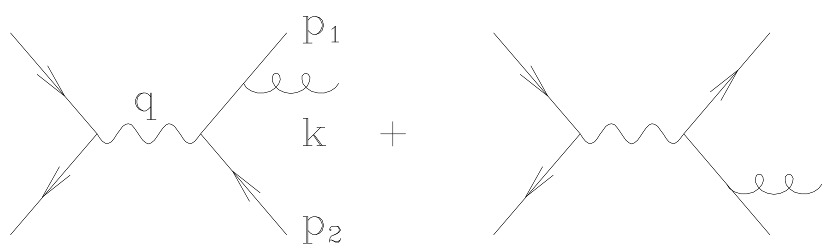

(b)

- Real emission diagrams (b):
  - Write 3-body phase-space integration as

$$d\Phi_3 = [...] d\alpha\, d\beta\, d\gamma\, dx_1\, dx_2 \ ,$$

α, β, γ are Euler angles of 3-parton plane,
$x_1 = 2p_1 \cdot q/q^2 = 2E_q/\sqrt{s}$,
$x_2 = 2p_2 \cdot q/q^2 = 2E_{\bar{q}}/\sqrt{s}$.

  - Applying Feynman rules and integrating over Euler angles:

$$\sigma^{q\bar{q}g} \ = \ 3\sigma_0 C_F \frac{\alpha_S}{2\pi} \int dx_1\, dx_2 \frac{x_1^2 + x_2^2}{(1-x_1)(1-x_2)} \ .$$

Integration region: $0 \le x_1, x_2, x_3 \le 1$ where $x_3 = 2k \cdot q/q^2 = 2E_g/\sqrt{s} = 2 - x_1 - x_2$.

- Integral divergent at $x_{1,2} = 1$:

$$
\begin{aligned}
1 - x_1 &= \tfrac{1}{2} x_2 x_3 (1 - \cos\theta_{qg}) \\
1 - x_2 &= \tfrac{1}{2} x_1 x_3 (1 - \cos\theta_{\bar{q}g})
\end{aligned}
$$

Divergences: collinear when $\theta_{qg} \to 0$ or $\theta_{\bar{q}g} \to 0$; soft when $E_g \to 0$, i.e. $x_3 \to 0$. Singularities are not physical – simply indicate breakdown of PT when energies and/or invariant masses approach QCD scale Λ.

- Collinear and/or soft regions do not in fact make important contribution to R. To see this, make integrals finite using dimensional regularization, with $D = 4 - 2\epsilon$ but $\epsilon < 0$ now. Then

$$
\sigma^{q\bar{q}g} = 2\sigma_0 \frac{\alpha_S}{\pi} H(\epsilon) \int dx_1 dx_2 \frac{(1-\epsilon)(x_1^2 + x_2^2) + 2\epsilon(1 - x_3)}{(1 - x_3)^\epsilon [(1 - x_1)(1 - x_2)]^{1+\epsilon}}
$$

where $$H(\epsilon) = \frac{3(1-\epsilon)(4\pi)^{2\epsilon}}{(3 - 2\epsilon)\Gamma(2 - 2\epsilon)} = 1 + \mathcal{O}(\epsilon)\ .$$

Hence

$$
\sigma^{q\bar{q}g} = 2\sigma_0 \frac{\alpha_S}{\pi} H(\epsilon) \left[\frac{2}{\epsilon^2} + \frac{3}{\epsilon} + \frac{19}{2} - \pi^2 + \mathcal{O}(\epsilon) \right] .
$$

- Soft and collinear singularities are regulated, appearing instead as poles at $D = 4$.

- Virtual gluon contributions (a): using dimensional regularization again

$$\sigma^{q\bar{q}} = 3\sigma_0 \left\{1 + \frac{2\alpha_S}{3\pi} H(\epsilon) \left[-\frac{2}{\epsilon^2} - \frac{3}{\epsilon} - 8 + \pi^2 + \mathcal{O}(\epsilon)\right]\right\} .$$

- Adding real and virtual contributions, poles cancel and result is finite as $\epsilon \to 0$:

$$R = 3 \sum_q Q_q^2 \left\{1 + \frac{\alpha_S}{\pi} + \mathcal{O}(\alpha_S^2)\right\} .$$

Thus R is an infrared safe quantity.

- Coupling α_S evaluated at renormalization scale μ. UV divergences in R cancel to $\mathcal{O}(\alpha_S)$, so coefficient of α_S independent of μ. At $\mathcal{O}(\alpha_S^2)$ and higher, UV divergences make coefficients renormalization scheme dependent:

$$R = 3\, K_{QCD} \sum_q Q_q^2 ,$$

$$K_{QCD} = 1 + \frac{\alpha_S(\mu^2)}{\pi} + \sum_{n\geq 2} C_n\left(\frac{s}{\mu^2}\right)\left(\frac{\alpha_S(\mu^2)}{\pi}\right)^n$$

- In $\overline{\mathrm{MS}}$ scheme with scale $\mu = \sqrt{s}$,

$$\begin{aligned} C_2(1) &= \frac{365}{24} - 11\zeta(3) - [11 - 8\zeta(3)]\frac{N_f}{12} \\ &\simeq 1.986 - 0.115 N_f \end{aligned}$$

  Coefficient C_3 is also known.

- Scale dependence of C_2, C_3 ... fixed by requirement that, order-by-order, series should be independent of μ. For example

$$C_2\left(\frac{s}{\mu^2}\right) = C_2(1) - \frac{\beta_0}{4}\log\frac{s}{\mu^2}$$

  where $\beta_0 = 4\pi b = 11 - 2N_f/3$.

- Scale and scheme dependence only cancels completely when series is computed to all orders. Scale change at $\mathcal{O}(\alpha_S^n)$ induces changes at $\mathcal{O}(\alpha_S^{n+1})$. The more terms are added, the more stable is prediction with respect to changes in μ.

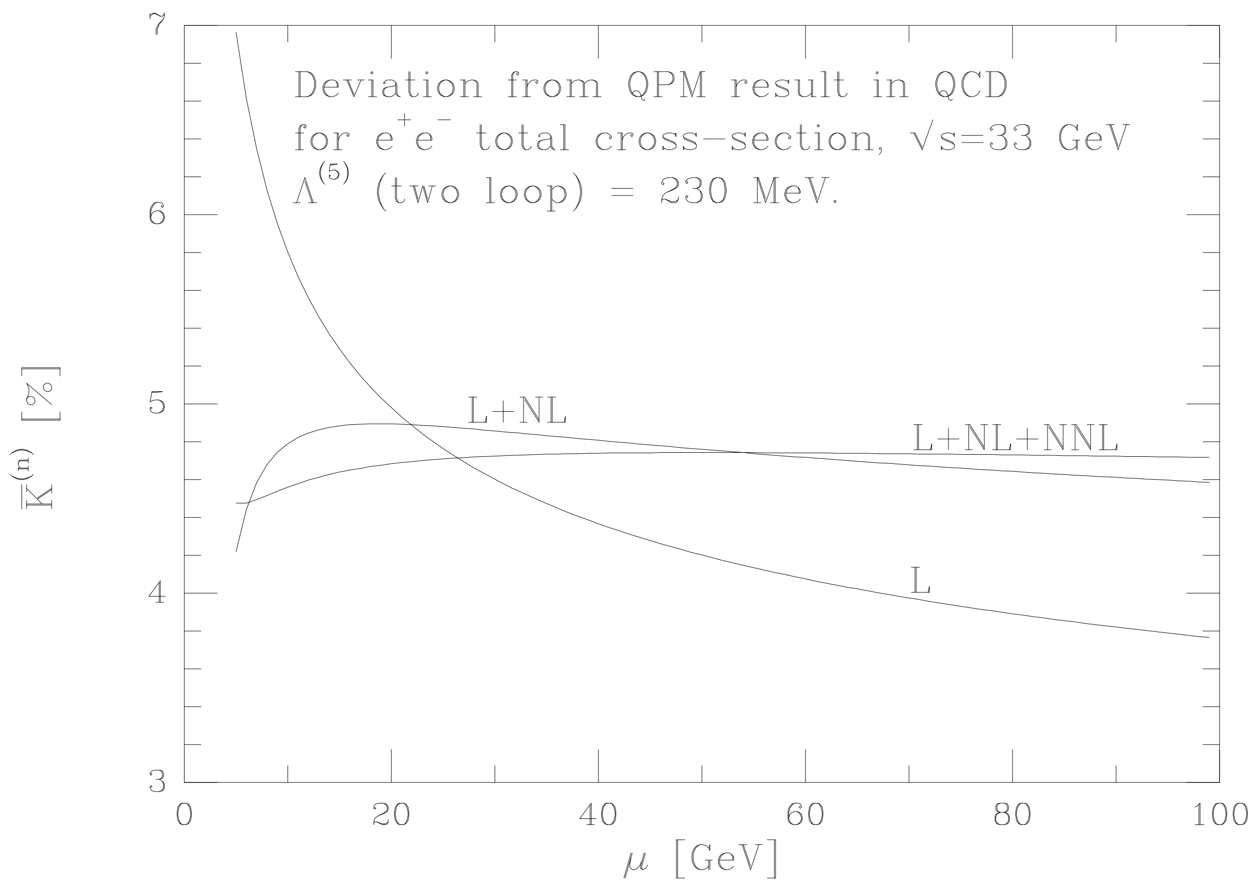

- Residual scale dependence is an important source of uncertainty in QCD predictions. One can vary scale over some 'physically reasonable' range, e.g. $\sqrt{s}/2 < \mu < 2\sqrt{s}$, to try to quantify this uncertainty. but there is no real substitute for a full higher-order calculation.

Shape distributions

- Shape variables measure some aspect of shape of hadronic final state, e.g. whether it is pencil-like, planar, spherical etc.
- For $d\sigma/dX$ to be calculable in PT, shape variable X should be infrared safe, i.e. insensitive to emission of soft or collinear particles. In particular, X must be invariant under $\boldsymbol{p}_i \to \boldsymbol{p}_j + \boldsymbol{p}_k$ whenever $\boldsymbol{p}_j$ and $\boldsymbol{p}_k$ are parallel or one of them goes to zero.
- Examples are Thrust and C-parameter:

$$
\begin{aligned}
T &= \max \frac{\sum_i |\boldsymbol{p}_i \cdot \boldsymbol{n}|}{\sum_i |\boldsymbol{p}_i|} \\
C &= \frac{3}{2} \frac{\sum_{i,j} |\boldsymbol{p}_i|\,|\boldsymbol{p}_j|\,\sin^2\theta_{ij}}{(\sum_i |\boldsymbol{p}_i|)^2}
\end{aligned}
$$

After maximization, unit vector $\boldsymbol{n}$ defines *thrust axis*.

- In Born approximation final state is $q\bar{q}$ and $1-T=C=0$. Non-zero contribution at $\mathcal{O}(\alpha_S)$ comes from $e^+e^- \to q\bar{q}g$. Recall distribution of $x_i = 2E_i/\sqrt{s}$:

$$\frac{1}{\sigma}\frac{d^2\sigma}{dx_1 dx_2} = C_F \frac{\alpha_S}{2\pi} \frac{x_1^2 + x_2^2}{(1-x_1)(1-x_2)} .$$

Distribution of shape variable X is obtained by integrating over x_1 and x_2 with constraint $\delta(X - f_X(x_1, x_2, x_3 = 2 - x_1 - x_2))$, i.e. along contour of constant X in (x_1, x_2)-plane.

- For thrust, $f_T = \max\{x_1, x_2, x_3\}$ and we find

$$\frac{1}{\sigma}\frac{d\sigma}{dT} = C_F \frac{\alpha_S}{2\pi}\left[\frac{2(3T^2-3T+2)}{T(1-T)}\log\left(\frac{2T-1}{1-T}\right) - \frac{3(3T-2)(2-T)}{(1-T)}\right] .$$

This diverges as $T \to 1$, due to soft and collinear gluon singularities. Virtual gluon contribution is negative and proportional to $\delta(1-T)$, such that correct total cross section is obtained after integrating over $\frac{2}{3} \leq T \leq 1$, the physical region for two- and three-parton final states.

- $\mathcal{O}(\alpha_S^2)$ corrections also known. Comparisons with data provide test of QCD matrix elements, through shape of distribution, and measurement of α_S, from overall rate. Care must be taken near $T = 1$ where (a) hadronization effects become large, and (b) large higher-order terms of the form $\alpha_S^n \log^{2n-1}(1-T)/(1-T)$ appear in $\mathcal{O}(\alpha_S^n)$.

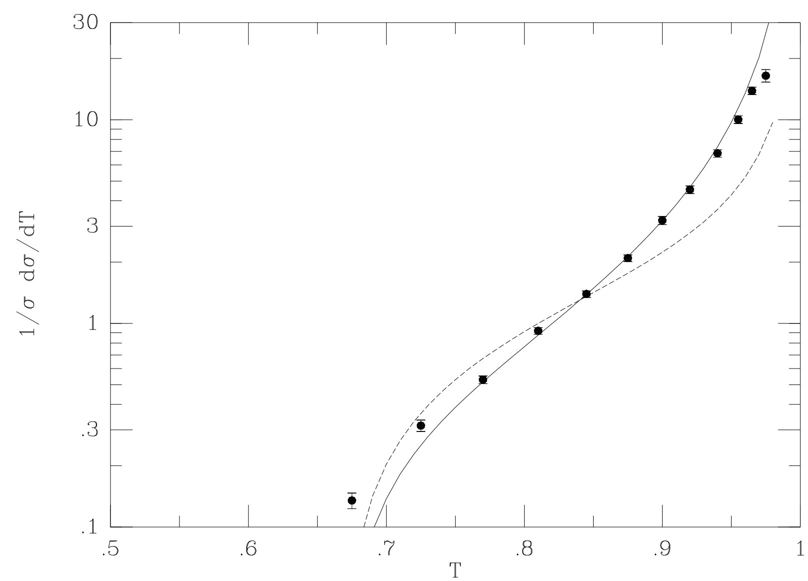

- Figure shows thrust distribution measured at LEP1 (DELPHI data) compared with theory for vector gluon (solid) or scalar gluon (dashed).

Jet fractions

- To define fraction f_n of n-jet final states ($n = 2, 3, \ldots$), must specify jet algorithm.
- Most common is k_T or Durham algorithm:
  - Define jet resolution $y_{\rm cut}$ (dimensionless).
  - For each pair of final-state momenta p_i, p_j define

$$y_{ij} = 2\min\{E_i^2, E_j^2\}(1 - \cos\theta_{ij})/s$$

  - If $y_{IJ} = \min\{y_{ij}\} < y_{\rm cut}$, combine I, J into one object K with $p_K = p_I + p_J$.
  - Repeat until $y_{IJ} > y_{\rm cut}$. Then remaining objects are jets.

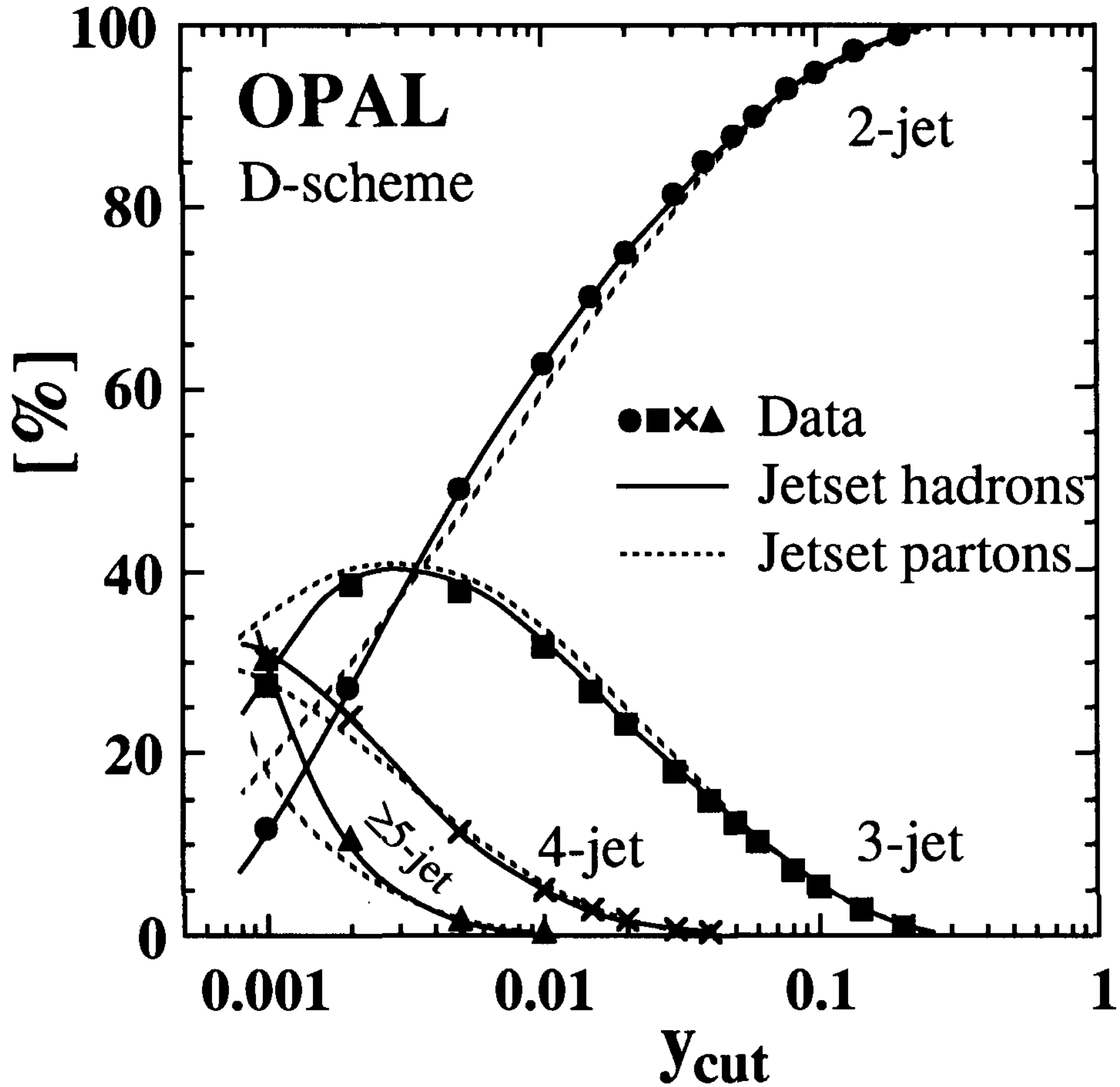
OPAL
D-scheme
100
80
60
40
20
0
[%]
0.001
0.01
0.1
1
ycut
Data
Jetset hadrons
Jetset partons
2-jet
3-jet
4-jet
≥5-jet

Parton branching

- Leading soft and collinear enhanced terms in QCD matrix elements (and corresponding virtual corrections) can be identified and summed to all orders. Consider splitting of outgoing parton a into $b + c$.

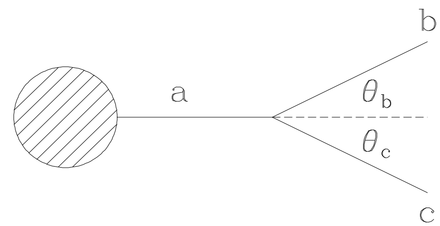

- Can assume $p_b^2, p_c^2 \ll p_a^2 \equiv t$. Opening angle is $\theta = \theta_a + \theta_b$, energy fraction is

$$z = E_b/E_a = 1 - E_c/E_a \ .$$

- For small angles

$$t = 2E_bE_c(1-\cos\theta) = z(1-z)E_a^2\theta^2 \ ,$$

$$\theta = \frac{1}{E_a}\sqrt{\frac{t}{z(1-z)}} = \frac{\theta_b}{1-z} = \frac{\theta_c}{z} \ .$$

- Consider first $g \to gg$ branching:
  - Amplitude has triple-gluon vertex factor

$$g f^{ABC} \epsilon_a^\alpha \epsilon_b^\beta \epsilon_c^\gamma [g_{\alpha\beta}(p_a - p_b)_\gamma + g_{\beta\gamma}(p_b - p_c)_\alpha + g_{\gamma\alpha}(p_c - p_a)_\beta]$$

    ϵ_i^μ is polarization vector for gluon i. All momenta defined as outgoing here, so $p_a = -p_b - p_c$. Using this and $\epsilon_i \cdot p_i = 0$, vertex factor becomes

$$-2g f^{ABC}[(\epsilon_a \cdot \epsilon_b)(\epsilon_c \cdot p_b) - (\epsilon_b \cdot \epsilon_c)(\epsilon_a \cdot p_b) - (\epsilon_c \cdot \epsilon_a)(\epsilon_b \cdot p_c)] \, .$$

  - Resolve polarization vectors into ϵ_i^{in} in plane of branching and ϵ_i^{out} normal to plane, so that

$$\begin{aligned} \epsilon_i^{\text{in}} \cdot \epsilon_j^{\text{in}} &= \epsilon_i^{\text{out}} \cdot \epsilon_j^{\text{out}} = -1 \\ \epsilon_i^{\text{in}} \cdot \epsilon_j^{\text{out}} &= \epsilon_i^{\text{out}} \cdot p_j \;\; = \;\; 0 \, . \end{aligned}$$

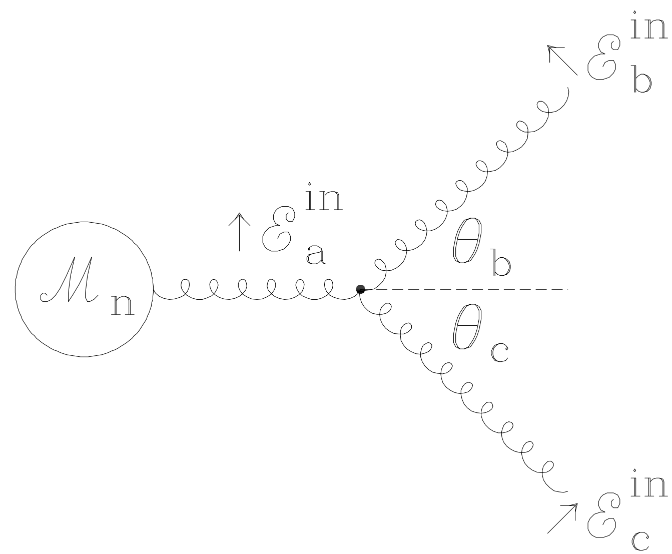

- For small θ, neglecting terms of order θ^2, we have

$$\begin{aligned}
\epsilon_a^{\rm in} \cdot p_b &= -E_b\theta_b = -z(1-z)E_a\theta \\
\epsilon_b^{\rm in} \cdot p_c &= +E_c\theta = (1-z)E_a\theta \\
\epsilon_c^{\rm in} \cdot p_b &= -E_b\theta = -zE_a\theta\ .
\end{aligned}$$

- Vertex factor proportional to θ, together with propagator factor of $1/t \propto 1/\theta^2$, gives $1/\theta$ collinear singularity in amplitude.
- $(n+1)$-parton matrix element squared (in small-angle region) is given in

terms of that for n partons:

$$|\mathcal{M}_{n+1}|^2 \sim \frac{4g^2}{t} C_A F(z;\epsilon_a,\epsilon_b,\epsilon_c) |\mathcal{M}_n|^2$$

where colour factor $C_A = 3$ comes from $f^{ABC} f^{ABC}$ and functions F are given below

ϵ_a	ϵ_b	ϵ_c	$F(z;\epsilon_a,\epsilon_b,\epsilon_c)$
in	in	in	$(1-z)/z + z/(1-z) + z(1-z)$
in	out	out	$z(1-z)$
out	in	out	$(1-z)/z$
out	out	in	$z/(1-z)$

- Sum/averaging over polarizations gives

$$C_A \langle F \rangle \equiv \hat{P}_{gg}(z) = C_A \left[\frac{1-z}{z} + \frac{z}{1-z} + z(1-z) \right] \, .$$

This is (unregularized) gluon splitting function.

- Enhancements at $z \to 0$ (b soft) and $z \to 1$ (c soft) due to soft gluon polarized in plane of branching.

- Correlation between polarization and plane of branching (angle ϕ):

$$F_\phi \propto \sum_{\epsilon_{b,c}} |\cos\phi\,\mathcal{M}(\epsilon_a^{\rm in},\epsilon_b,\epsilon_c) + \sin\phi\,\mathcal{M}(\epsilon_a^{\rm out},\epsilon_b,\epsilon_c)|^2$$

$$\propto \frac{1-z}{z} + \frac{z}{1-z} + z(1-z) + z(1-z)\cos 2\phi\,.$$

  Hence branching in plane of gluon polarization preferred.

- Consider next $g \to q\bar{q}$ branching:
  - Vertex factor is

$$-ig\bar{u}^b\gamma_\mu\epsilon_a^\mu v^c$$

  where u^b and v^c are quark and antiquark spinors.

  - Spin-averaged splitting function is

$$T_R\,\langle F\rangle \equiv \hat{P}_{qg}(z) = T_R\left[z^2 + (1-z)^2\right]\,.$$

  No soft ($z \to 0$ or 1) singularities since these are associated only with gluon emission.

  - Vector quark-gluon coupling implies (for $m_q \simeq 0$) q and $\bar{q}$ helicities always opposite (helicity conservation).

- Correlation between gluon polarization and plane of branching:

$$F_\phi = z^2 + (1-z)^2 - 2z(1-z)\cos 2\phi$$

  i.e. strong preference for splitting perpendicular to polarization.

- Branching $q \to qg$:
  - Spin-averaged splitting function is

$$C_F \langle F \rangle \equiv \hat{P}_{qq}(z) = C_F \frac{1+z^2}{1-z} \, .$$

  - Helicity conservation ensures that quark does not change helicity in branching.
  - Gluon polarized in plane of branching preferred, polarization angular correlation being

$$F_\phi = \frac{1+z^2}{1-z} + \frac{2z}{1-z} \cos 2\phi \, .$$

Phase space

- Phase space factors before and after branching are related by

$$d\Phi_{n+1} = d\Phi_n \frac{1}{4(2\pi)^3} dt\, dz\, d\phi \, .$$

- Hence cross sections before and after branching are related by

$$d\sigma_{n+1} = d\sigma_n \frac{dt}{t} dz \frac{d\phi}{2\pi} \frac{\alpha_{\rm S}}{2\pi} C F$$

where C and F are colour factor and polarization-dependent z-distribution introduced earlier. Integrating over azimuthal angle gives

$$d\sigma_{n+1} = d\sigma_n \frac{dt}{t} dz \frac{\alpha_{\rm S}}{2\pi} \hat{P}_{ba}(z) \, .$$

where $\hat{P}_{ba}(z)$ is $a \to b$ splitting function.

4-jet angular distribution

- Angular correlations are illustrated by the angular distribution in $e^+e^- \to 4$ jets. Bengtsson-Zerwas angle χ_{BZ} is angle between the planes of two lowest and two highest energy jets:

$$\cos\chi_{BZ} = \frac{(\boldsymbol{p}_1 \times \boldsymbol{p}_2) \cdot (\boldsymbol{p}_3 \times \boldsymbol{p}_4)}{|\boldsymbol{p}_1 \times \boldsymbol{p}_2|\,|\boldsymbol{p}_3 \times \boldsymbol{p}_4|}\ .$$

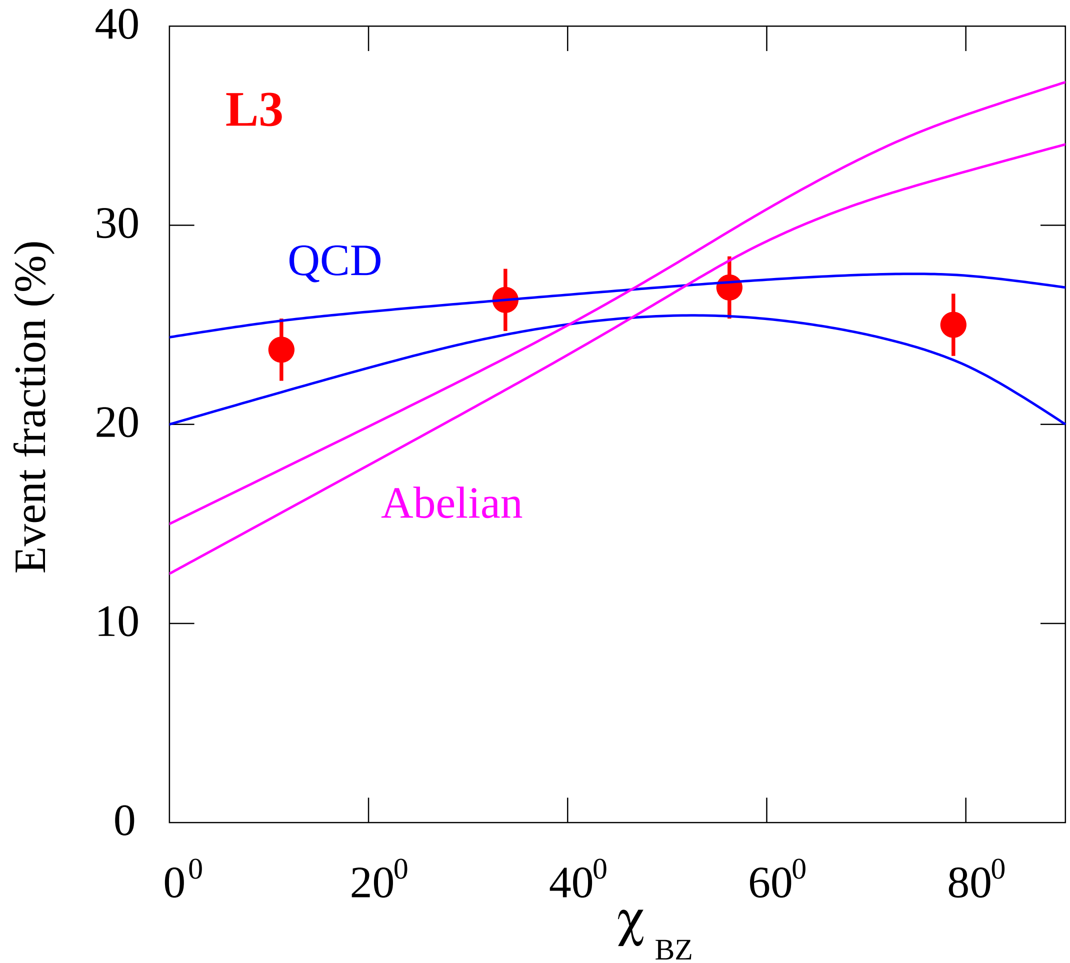

- Lowest-order diagrams for 4-jet production shown below. Two hardest jets tend to follow directions of primary $q\bar{q}$.

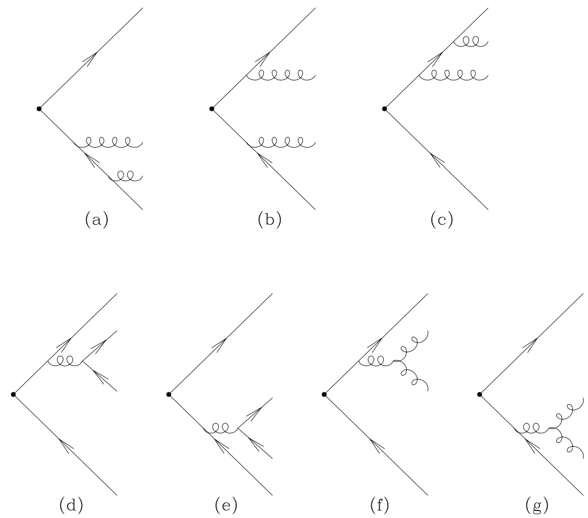

- “Double bremsstrahlung” diagrams give negligible correlations.
- $g \to q\bar{q}$ give strong anti-correlation (“Abelian” curve), because gluon is polarized in plane of primary jets and prefers to split $\perp^{r}$ to polarization.
- $g \to gg$ occurs more often parallel to polarization. Although its correlation is much weaker than in $g \to q\bar{q}$, $g \to gg$ is dominant in QCD due to larger colour factor and soft gluon enhancements.
- Thus B-Z angular distribution is flatter than in an Abelian theory.

Summary of Lecture 2

- e^+e^- hadronic total cross section, event shapes and jet fractions are infrared safe quantities which can be predicted using QCD perturbation theory.
- Parton branching approximation describes collinear-enhanced contribution to multi-parton cross sections in terms of splitting functions $P_{ij}(z)$.
- $e^+e^- \to$ 4-jet distributions show angular correlations due to spin of the gluon.